A Low Power Wireless Power Transfer Prototype Design and Implementation

Furkan Ozturk[1,2], Sinan Kivrak[1], and M. Timur Aydemir[2]

[1]Ankara Yildirim Beyazit University, Etlik, Ankara
fozturk.ybu@gmail.com, sinan.kivrak@hotmail.com
[2]Gazi University, Maltepe, Ankara
aydemirmt@gazi.edu.tr

Abstract

Wireless Power Transfer has become feasible recently and there have been several research projects to apply this concept in various areas, including electric vehicle battery charging. Contactless charging of batteries is a desired method as it avoids the hassle and dirt associated with cables and enables flexibility. In this paper a low power prototype to transfer about 100 W across 5 cm distance is presented. The operating frequency 19.23 kHz and the achieved efficiency is about 82%. Design steps, simulation results and test results are given and discussed.

Keywords: Wireless power transfer, series-series resonance circuit

1. Introduction

Wireless Power Transfer (WPT) has been an exciting subject since it was first put forward by Tesla in 1891. WPT is the transfer of energy from a source to a load without any mechanical connection between them. Some of the most important problems encountered with mechanical connections (plugs, cables, etc.) are corrosion caused by airborne moisture and dust, resulting in physical movements. Thanks to WPT, these problems can easily be overcome. Since it can be used in a variety of environments other than just dry environments, such as underwater, it attracts a lot of interest in several industrial applications.

Today, the use of electric vehicles is becoming increasingly widespread. The most important reason for this is the increasing drive range of electric vehicles with a single charge. This has become possible with the development in battery technology. One of the obstacles in front of increased use is the charging time of batteries. One of the ways to shorten the long charging times is to perform the charging at high current.

When charging is carried out by cable, several main problems may occur. The primary problem among these is security. As a result of the fast charging process, a high current flows through the connection cable, which carries the intermediary connection. Serious problems may occur when the short circuit at the connection point or the connection cable. The second problem is the erosion caused by the environment. The mechanical connections can be easily influenced by the environment. As a result of moisture, dust, etc., corrosion may occur at the connection points. The third problem is the need to wait for the car's charging needs during long-distance trips.

Charging with WPT technology has the potential to overcome these problems. The battery can be fed with high current without any mechanical connection with the source. Since it is an enclosed and secure layer of protection, it is not affected by the outside environment, and there is no negative impact on the connection points. In the motorway projects developed for the long distance use of electric vehicles, with the help of WPT technology, the charging requirements of the vehicles are realized while the vehicle is traveling, providing uninterrupted travel. Furthermore, the spread of the applied highway WPT charging technology can reduce the battery capacity in vehicles. In this way, it is possible to realize the expansion of electric vehicles by reducing expensive battery supply and maintenance fees.

Alanson P. Sample and his friends have demonstrated both theoretical and experimental work in the field [1]. They also developed a system that can operate with an efficiency up to 70% at 0 cm - 70 cm range [2]. In his model, the value of the load is kept constant, showing that the system runs at high efficiency in various air gaps. The operating frequency was chosen to be 7.6 MHz. This value was selected based on the critical coupling coefficient. This is the point where the frequency begins to divide. At the same time, impedance compensation is performed using adaptive frequency.

Seung-Hwan Lee, in his work, used a 3.7 MHz operating frequency [3]. In his experiment, he performed wireless power transmission of 220 W with 95% efficiency at 30 cm air gap. He states that the spatial distribution of current and voltage will not change over the circuit elements if the characteristic length of the windings is sufficiently smaller than the relevant wavelength. For this reason, while the design of the windings is carried out, the wavelength is included in calculations. After performing the experiment with traditional winding methods, he developed new winding techniques and concentrated on the high frequency resistance values of the windings. In this new technique, it has succeeded in reducing the high frequency internal resistance (ESR resistance) of the windings.

In a high-frequency system the operating frequency of about 13.5 MHz was used in [4]. Frequency scanning was performed at various air gaps (49 mm - 357 mm) to determine the point at which maximum efficiency was achieved. At the same time, the value of the coupling between these windings was interpreted.

A detailed analysis and design method is given in [5] for an operating frequency of 20 kHz. A prototype circuit was built with an efficiency of 82% at a distance of 15 cm between windings having 2 kW power. An iterative algorithm that can be used in winding design is presented. The algorithm starts with the selection of winding geometry. The air-gap distance between the windings, desired power and initial frequency are recorded as initial values in the algorithm. Then the algorithm is executed to complete the design. Possible solutions generated at each iteration are evaluated and the most proper solution is chosen. A new design factor, "KD", in the design is presented.

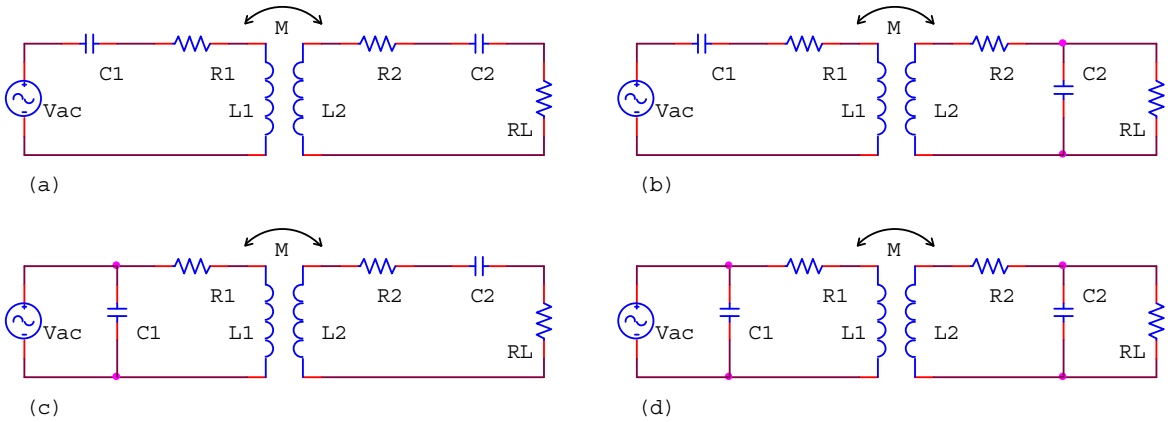

Fig. 1. The main resonance topologies, (a) SS, (b) SP, (c) PS, (d) PP

Wireless transmission of 6.6 kW through a 12 cm to 20 cm air gap to charge the battery of an electric vehicle was reported in [6]. The operating frequency is 20.3 kHz. Bidirectional power transfer was possible in this system and communication existed between the source side and the load side. This made it possible to control the frequency and allow self-resonance PWM (SR-PWM). The frequency control ensures that the windings are always at resonant.

Operating frequencies of 20 kHz and 85 kHz were used in [7]. Serial-serial resonance is chosen as the circuit topology.

A 300 kW system is described in [8] for rail road applications. The air gap was selected as 7 cm at an operating frequency of 60 kHz.

The highest power transferred without any contact was reported in [9]. The system with 1 MW of power has an efficiency of 82.7%. The air gap between the windings is 5 cm and the operating frequency is 60 kHz. This system was tested on a fast train and the results show that wireless power transmission can be used for vehicles with high power.

In this paper, analysis, design and implementation of a low power Series-Series Resonant WPT prototype is presented. 100 W power was transferred through an air-gap of 5 cm with an operating frequency of 20 kHz.

2. WPT Topologies

There are four main KGA topologies: Serial-Serial Resonance Circuit, Serial-Parallel Resonance Circuit, Parallel-Serial Resonance Circuit and Parallel-Parallel Resonance Circuit. The terms in the topologies refer to the way the resonance capacitors in the circuit are connected to the windings. These four basic circuit topologies are shown in Fig.1.

The circuit parameters, current and voltage phasors used in the design equations are as given in Fig. 2. The side where the source is will be called the primary side, and the side where the load is will be called the secondary side.

The Kirchhoff's Voltage Law (KVL) applied on the primary and secondary sides yields

$$V_s - I_1\left[R_1 + j\left(\omega L_1 - \frac{1}{\omega C_1}\right)\right] - I_2(j\omega M) = 0 \qquad (1)$$

$$I_2\left[(R_2 + R_L) + j\left(\omega L_2 - \frac{1}{\omega C_2}\right)\right] - I_1(j\omega M) = 0 \qquad (2)$$

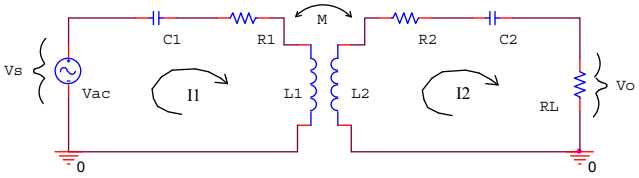

Fig. 2. Series-series resonance circuit

Equation (1) and Equation (2) are solved to obtain

$$V_s - I_1\left[R_1 + j\left(\omega L_1 - \frac{1}{\omega C_1}\right) + \frac{\omega^2 M^2}{(R_2 + R_L) + j\left(\omega L_2 - \frac{1}{\omega C_2}\right)}\right] = 0 \qquad (3)$$

Impedance value seen by the source is defined as

$$Z = \frac{V_S}{I_1} \qquad (4)$$

and is obtained as

$$Z = R_1 + j\left(\omega L_1 - \frac{1}{\omega C_1}\right) + \frac{\omega^2 M^2}{(R_2 + R_L) + j\left(\omega L_2 - \frac{1}{\omega C_2}\right)} \qquad (5)$$

In order for the maximum amount of power to be transferred to load, the imaginary value of the impedance seen by the source must be zero. Thus,

$$\mathrm{Im}\{Z\} = \mathrm{Im}\left\{R_1 + j\left(\omega L_1 - \frac{1}{\omega C_1}\right) + \frac{\omega^2 M^2}{(R_2 + R_L) + j\left(\omega L_2 - \frac{1}{\omega C_2}\right)}\right\} = 0 \qquad (6)$$

As can be seen in Equation (6) to achieve this is to make

$$\omega L_1 = \frac{1}{\omega C_1} \quad , \quad \omega L_2 = \frac{1}{\omega C_2} \qquad (7)$$

The simplest method to implement this with a single operating frequency is to set $L_1 = L_2$, $C_1 = C_2$. With these assumptions, when the Equation (7) is solved, we have,

$$\omega = \frac{1}{\sqrt{L_1 C_1}} \tag{8}$$

The angular frequency is

$$\omega = 2\pi f \tag{9}$$

The frequency in terms of circuit parameters can be shown as

$$f = \frac{1}{2\pi\sqrt{L_1 C_1}} \tag{10}$$

If the capacitor selection is done properly, the imaginary part of the input impedance is eliminated and unity power factor operation is achieved at the resonant frequency.

$$\mathrm{Re}\{Z\} = \mathrm{Re}\left\{R_1 + j\left(\omega L_1 - \frac{1}{\omega C_1}\right) + \frac{\omega^2 M^2}{(R_2 + R_L) + j\left(\omega L_2 - \frac{1}{\omega C_2}\right)}\right\} \tag{11}$$

$$\mathrm{Re}\{Z\} = R_1 + \frac{4\pi^2 f^2 M^2}{R_2 + R_L} \tag{12}$$

Active power given to the circuit at this frequency is

$$P_a = {I_1}^2 \mathrm{Re}\{Z\} \tag{13}$$

Equation (13) shows that the active power given to the circuit is directly proportional with the frequency.

The power transmitted to the load is given as

$$P_L = {I_2}^2 R_L \tag{14}$$

The efficiency is in the simplest sense that;

$$\eta = \frac{P_L}{P_s} = \frac{{I_2}^2 R_L}{V_s I_1} \tag{15}$$

The turn numbers of the windings are calculated after the power to be transmitted in the circuit is determined and the operating frequency is decided. The dimensions of the windings and the number of turns must be proper to yield the desired flux density. This is an iterative process which is repeated until the desired flux density is obtained. The self and mutual inductance values of the windings are calculated by using Neumann's formula as given Equation (16) and (17).

$$L = \frac{\mu_0}{4\pi} N^2 \oint_{\gamma_1} \oint_{\gamma_2} \frac{dl.\, dl'}{r} \tag{16}$$

$$M = \frac{\mu_0}{4\pi} N_1 N_2 \oint_{\gamma_1} \oint_{\gamma_2} \frac{dl.\, dl'}{r} \tag{17}$$

3. Design and Test of the Prototype Circuit

The parameters of the prototype system implemented in this work are given in Table 1.

In order to design this prototype all design equations were evaluated in a MATLAB code. The iterative algorithm yields results as explained before and at the end optimum design parameters are obtained. Table 2 lists the circuit components and their values obtained by running the code.

Table 1. Desired Circuit Values

Parameter	Value
Desired Power (W)	100
Source Voltage (VDC)	20
Air Gap (cm)	5
Operating Frequency (kHz)	20

It is always a good practice to simulate the circuit before actually building it. The simulation was carried out in Pspice to see if the parameters obtained in MATLAB calculations were proper. Some simulation results are shown in Fig. 3.

Table 2. Prototype Circuit Values

Parameter	Prototype Circuit Value
Source Voltage (VDC)	20
Air Gap (cm)	5
Operating Frequency (kHz)	19.23
N1	11
N2	14
Primary winding geometry (m x m)	0.3 x 0.3
Secondary winding geometry (m x m)	0.2 x 0.2
Cross Sectional Area (mm^2)	2.5
$L_1(\mu H)$	99.15
$L_2(\mu H)$	98.98
$C_1(nF)$	1000
$C_2(nF)$	1000
$R_L(\Omega)$	2.5

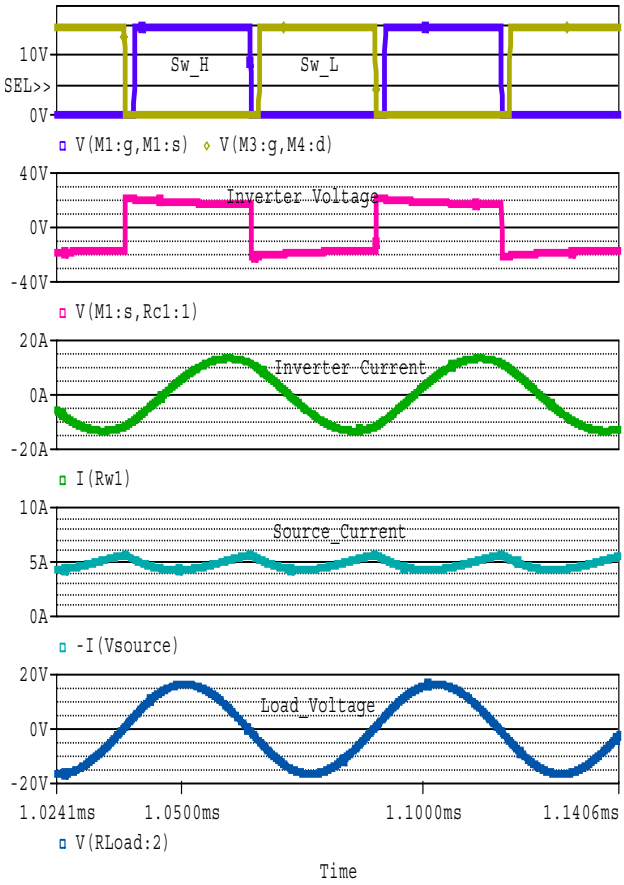

Fig. 3. Simulation result

The designed prototype was implemented in the laboratory as seen in Fig. 4.

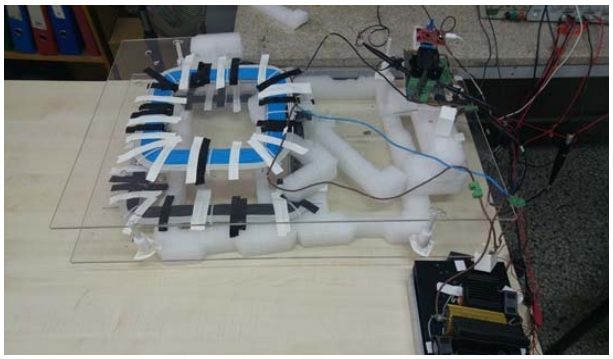

Fig. 4. Prototype circuit

The switching signals given to the microprocessor are adjustable. Operating frequency was dynamically changed while the program was running to determine the point at which maximum power was transferred.

Figures 5-7 show experimental results. In Fig.5 are given the inverter output signals. The peak value of the current is 9 A.

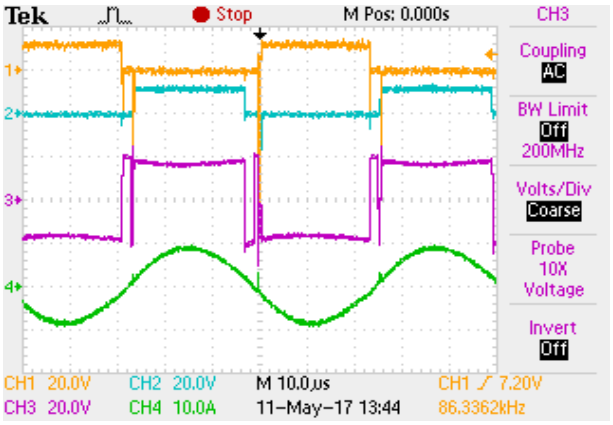

Fig. 5. Output of DC/AC converter

In Fig. 6, the voltage, current and instant power on the load in the prototype circuit are given. The output voltage of peak value is about 20 V and output current peak value is about 8 A. The output average power value is 79.3W.

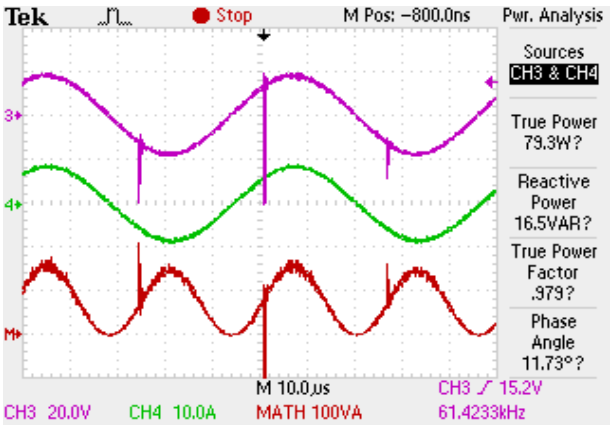

Fig. 6. Voltage, current and power of load

In the Fig. 7, the voltage, current and instant power on the source in the prototype circuit are given. The input voltage is about 20 V and input current value is 5 A. The input average power value which is 96.6 W and the efficiency is calculated as 82.1%.

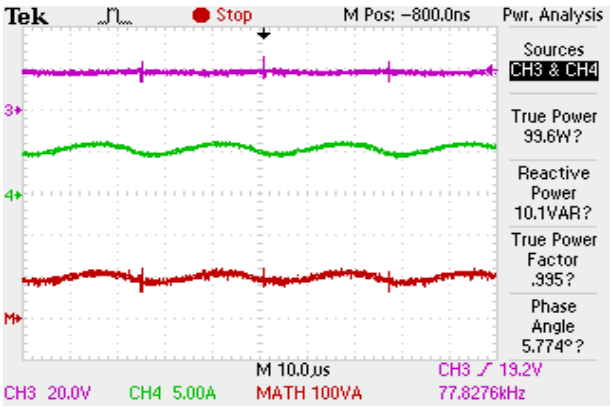

Fig. 7. Voltage, current and power at the source

The prototype was tested with different input voltage values. Table 3 shows the results of these tests. In general, the efficiency is between 60-70%. The input voltage is limited to 40 V to safely test the system. Maximum efficiency of 82.1% is attained at 20 V input since the design was carried out for this voltage.

Table 3. The results of circuit for various source voltages

Source Voltage (V)	Source Power (W)	Transferred Power (W)	Efficiency (%)
10,00	27,30	19,00	69,60
20,00	99,60	79,30	82,09
30,00	235,00	143,00	60,85
40,00	414,60	263,00	63,43

Effect of different air-gap distances was also tested and the results are given in Table 4. The frequency was kept constant at 19.23 kHz and the source voltage is fixed to 20 V. The efficiency drops as the air gap increases, as expected.

Table 4. The results of circuit for various air gaps

Air Gap (cm)	Source Power (W)	Transferred Power (W)	Efficiency (%)
5,0	99,60	79,30	82,09
7,5	102,60	57,10	55,65
10,0	72,18	36,00	49,88
12,5	47,00	20,30	43,19

4. Conclusion

Wireless Power Transfer is a technology that has great importance especially for electric vehicles. WPT has the ability to provide solutions to many problems of electric vehicles.

In this work, a low power prototype has been designed, implemented and tested. Design process, simulation results and test results are given for a series-series compensated topology. A maximum efficiency near 82% was obtained. Higher efficiency values can be reached if the power level is increased. The work is continuing to improve the prototype and test it at higher powers with other compensation topologies.

5. References

[1] A.P. Sample, D.A. Meyer, J.R. Smith, "Analysis Experimental Results and Range Adaptation of Magnetically Coupled Resonators for Wireless Power Transfer", *Industrial Electronics IEEE*, vol. *58*, no. *2*, pp. *544-554*, 2011.

[2] A.P. Sample, J.R. Smith, "Wireless Power Transfer Apparatus and Method Thereof", *U.S. Patent US8299652B2*, 2012.

[3] S.H. Lee, R.D. Lorenz, "Development and Validation of Model for 95%-Efficiency 220-W Wireless Power Transfer Over a 30-cm Air Gap", *IEEE Trans. Ind. Appl.*, vol. *47*, no. *6*, pp. *2495-2504*, 2011.

[4] T. Imura, Y. Hori, "Maximizing Air Gap and Efficiency of Magnetic Resonant Coupling for Wireless Power Transfer Using Equivalent Circuit and Neumann Formula", *IEEE Trans. On Industrial Electronics*, vol. *58*, no. *10*, pp. *4746-4752*, 2011.

[5] J. Sallan, J.L. Villa, A. Llombart, J.F. Sanz, "Optimal Design of ICPT Systems Applied to Electric Vehicle Battery Charge", *IEEE Trans. On Industrial Electronics,* vol. *56,* no. *6,* pp. *2140-2149*, 2009.

[6] J.Y. Lee, "A Bidirectional Wireless Power Transfer EV Charger Using Self-Resonant PWM", *IEEE Trans. On Power Electronics*, vol. *30*,no. *4*, pp. *1784-1787*, 2015.

[7] B. Yang, S. Du, W. Chen, C. Deng, D. Xu, "Optimal parameters design for series-series resonant converter for wireless power transfer", *Proc. Int. Power Electron. Appl. Conf. Expo.*, 772-777, 2014.

[8] S.H. Lee, B.S. Lee, J.H. Lee, C.B. Park, S.G. Lee, S.M. Jung, et al., "A New Design Methodology for a 300-kW, Low Flux Density, Large Air Gap, Online Wireless Power Transfer System", *IEEE Transactions on Industry Applications*, vol. *52*, no. *5*, pp. *4234-4242*, 2016.

[9] J.H. Kim, B.S. Lee, J.H. Lee, S.H. Lee, C.B. Park, S.M. Jung, et al., "Development of 1-MW Inductive Power Transfer System for a High-Speed Train", *IEEE Trans. On Industrial Electronics*, vol. *62*, no. *10*, pp. *6242-6250*, 2015.